HHS Public Access

Author manuscript

Mol Pharm. Author manuscript; available in PMC 2023 March 07.

Published in final edited form as:

Mol Pharm. 2022 March 07; 19(3): 775–787. doi:10.1021/acs.molpharmaceut.1c00373.

Antibodies with weakly basic isoelectric points minimize trade-offs between formulation and physiological colloidal properties

Priyanka Gupta[1,5], **Emily K. Makowski**[3,4], **Sandeep Kumar**[5], **Yulei Zhang**[3,4], **Justin M. Scheer**[5,6], **Peter M. Tessier**[1,2,3,4,*]

[1]Biochemistry and Biophysics Department, Rensselaer Polytechnic Institute, Troy, NY 12180, USA,

[2]Department of Pharmaceutical Sciences, Biointerfaces Institute, University of Michigan, Ann Arbor, MI 48109, USA,

[3]Department of Chemical Engineering Biointerfaces Institute, University of Michigan, Ann Arbor, MI 48109, USA,

[4]Department of Biomedical Engineering, Biointerfaces Institute, University of Michigan, Ann Arbor, MI 48109, USA,

[5]Biotherapeutics Molecule Discovery Department, Boehringer Ingelheim Pharmaceuticals Inc., Ridgefield, CT 06877, USA,

[6]Janssen R&D, South San Francisco, CA 94080, USA

Abstract

The widespread interest in antibody therapeutics has led to much focus on identifying antibody candidates with favorable developability properties. In particular, there is broad interest in identifying antibody candidates with highly repulsive self-interactions in standard formulation conditions (e.g., low ionic strength buffers at pH 5–6) for high solubility and low viscosity. Likewise, there is also broad interest in identifying antibody candidates with low levels of non-specific interactions in physiological conditions (PBS, pH 7.4) to promote favorable pharmacokinetic properties. To what extent antibodies can be systematically identified that possess both highly repulsive self-interactions in standard formulation conditions and weak non-specific interactions in physiological conditions remains unclear and is a potential impediment to successful therapeutic drug development. Here we evaluate these two properties for 42 IgG1 variants based on the variable fragments (Fvs) from four clinical-stage antibodies and complementarity-determining regions from ten clinical-stage antibodies. Interestingly, we find that antibodies with the strongest repulsive self-interactions in a standard formulation condition (pH 6 and 10 mM histidine) display the strongest non-specific interactions in physiological conditions. Conversely, antibodies with the weakest non-specific interactions in physiological conditions display the least repulsive self-interactions in standard formulations. This behavior can be largely explained by the antibody isoelectric point, as highly basic antibodies that are

*corresponding author (ptessier@umich.edu).

CONFLICTS OF INTEREST

P.G., J.M.S. and S.K. were employees of Boehringer Ingelheim Pharmaceuticals Inc when this research was conducted.

highly positively charged at standard formulation conditions (pH 5–6) promote repulsive self-interactions that mediate high antibody stability but also mediate strong non-specific interactions with negatively charged biomolecules at physiological pH, and vice versa for antibodies with negatively charged Fv regions. Therefore, IgG1s with weakly basic isoelectric points between 8–8.5, and Fv isoelectric points between 7.5–9, typically display the best combinations of strong repulsive self-interactions and weak non-specific interactions. We expect that these findings will improve the identification and engineering of antibody candidates with drug-like biophysical properties.

Keywords

developability; specificity; non-specific; nonspecific; polyreactivity; off-target binding; colloidal stability; self-association; self-interactions; non-specific interactions; Fv net charge; Fv isoelectric point

INTRODUCTION

Monoclonal antibodies (mAbs) are currently the dominant class of biotherapeutics used for the treatment of indications related to oncology, immune modulation, respiratory disorders, inflammation, and ophthalmology.[1–5] Currently there are over ninety approved antibody therapeutics[6] and their success is attributed to several of their key properties, including their high specificity and affinity, low non-mechanistic toxicity, long half-life and high stability compared to other biologics.[7, 8] Despite this success, attrition rates for mAbs before approval remains significantly high, which strongly contributes to the high cost of therapeutic antibody development. Early identification of antibodies with optimal drug-like properties is essential to reduce the likelihood of failures in the clinic.

Two antibody properties – namely antibody non-specific and self-interactions – are both of significant importance for successful antibody drug development.[9, 10] Antibody non-specific interactions in physiological conditions lead to off-target binding, non-specific cellular uptake, intracellular degradation and/or abnormal interactions with FcRn, which increase the risk for fast antibody clearance and poor efficacy *in vivo*.[11–17] Antibody self-association in standard formulation conditions (low ionic strength formulations at pH 5–6) can lead to poor solubility, opalescence and high viscosity in concentrated antibody formulations, which increases the risk for poorly stable and viscous antibody formulations that are unsuitable for subcutaneous delivery.[10, 18–27]

While it is desirable to identify antibodies with both low non-specific interactions and low self-association, a holistic analysis of previous studies of each individual property suggests that this may be particularly challenging. For example, strongly positively-charged antibodies with high isoelectric points have been shown to display low risk for high self-association, viscosity and opalescence in standard formulation conditions.[20, 28–30] However, the same type of strongly positively-charged antibodies have also been shown to display high risk for non-specific interactions in physiological conditions (pH 7.4, PBS) and fast antibody clearance *in vivo*.[14, 31–40] Likewise, strongly negatively charged antibodies with low isoelectric points have been shown to display high risk for high self-association,

viscosity and opalescence in standard formulation conditions, while the same antibodies display low-to-medium risk for non-specific interactions in physiological conditions and fast antibody clearance *in vivo*.[22, 25–27, 39, 41–43]

Despite these important previous studies, there has been little systematic evaluation of these trade-offs and much remains unknown about how to identify antibodies with optimal combinations of both properties. Here we have sought to directly evaluate trade-offs between antibody non-specific binding (pH 7.4, PBS) and self-association (pH 6, 10 mM histidine) for a panel of antibodies with systematic variation in physicochemical properties of their frameworks and main binding loops (heavy chain CDR3) using the Fv frameworks from four clinical-stage antibodies and the heavy chain CDR3s from ten clinical-stage antibodies (Fig. 1). In particular, we have evaluated the contributions of antibody charge, hydrophobicity, and other physicochemical properties to antibody self-association and non-specific binding. Herein, we report surprisingly strong trade-offs between antibody non-specific binding and self-association, and optimal ranges of antibody physiochemical properties for identifying favorable antibodies with low levels of both non-specific binding and self-association.

METHODS AND MATERIALS

Cloning of antibody variants

The heavy (V_H) chain variable genes with grafted heavy CDR3 (HCDR3) sequences and the parent antibody heavy and light (V_K) chain genes along with the leader sequence were synthesized as gene blocks (IDT technologies). Both V_H and V_K gene blocks were cloned using HindIII and EcoRI restriction sites seamlessly with InFusion enzyme mix into pTT5 vectors carrying the IgG1 and kappa constant genes respectively. Sequence confirmed vector constructs of the variant antibodies were scaled up to prepare endotoxin free plasmid DNA for expression in CHO-3E7 (CHO-E) mammalian cell line (L-11992, National Research Council Canada). All the variable genes were designed with codons for optimal mammalian expression.

Expression and purification of antibody variants

The recombinant antibodies were transiently expressed using optimized methods reported previously.[67] Briefly, CHO-E cells maintained in Glutamax supplemented FreeStyle CHO media at 37 °C, 5% CO_2, and 150 rpm shake speed were used for transient transfection. Prior to transfection the cells were seeded at a cell density of 2 million cells per mL in 400 mL of BalanCD Transfectory CHO media supplemented with 4 mM L-glutamine. The heavy chain (0.075 mg) and light chain (0.15 mg) plasmids were mixed at 1:2 ratio along with 70% filler DNA (0.525 mg) making it a total of 0.75 mg of DNA into 50 mL of OptiPro media and sterilized by vacuum filtration. Half the volume (0.375 mL) of TransIT-PRO transfection reagent was added to the DNA-OptiPro transfection solution and gently swirled to mix. The DNA-TransIT-Pro complex media was added immediately to the flask containing the cells with gentle swirl. The shake flasks were transferred to orbital shaker at 140 rpm at 37 °C and 5% CO_2. Four hours post transfection, 50 mL Transfectory Supplement (12.5% culture volume) and 1.0 mL Anti-Clumping agent (Gibco) were added, and the temperature shifted

to 30 °C. Between days 5 to 7 post-transfection, 50 ml of CHO Feed B media was added to the transfected cells to maintain the glucose titer >2 gm/L. The transfected cultures were maintained for 8–9 d and harvested by centrifuging at 4700 rpm, 4 °C for 40 min, followed by sterile filtration through a 0.2 μm filter.

The harvested supernatants were subjected to parallel Protein A affinity chromatography using the Protein Maker system (Protein BioSolutions). Sample and buffer lines were cleaned with 0.5 M NaOH to remove any contaminants and equilibrated in DPBS (8.05 mM sodium phosphate, 137 mM NaCl, 1.47 mM potassium phosphate, 2.6 mM potassium chloride, pH 7.2). The column was equilibrated with ten column volumes of DPBS at a speed of 5 mL/min. The supernatant with recombinant antibody was loaded on to a 5 mL HiTrap MabSelect SuRe™ column (GE Healthcare) at a flow rate of 0.5 mL/min overnight and then washed with ten column volumes of DPBS. The column was then subjected to high salt wash using 1 M NaCl followed by another DPBS wash both with ten column volumes at a flow rate of 5 mL/min. Before eluting the antibody, the column was subjected to pre-elution with 3 mL of 30 mM sodium acetate pH 3.5. The bound antibody was then eluted off the column with 5 mL of 30 mM sodium acetate pH 3.5 at a flow rate of 1 mL/min and immediately neutralized with 1% by volume using 3 M sodium acetate pH 9.0 to bring the final formulation to 60 mM sodium acetate pH 5.0. The elution and neutralization steps were repeated two more times to ensure all the bound antibody was eluted off the column. The concentration in the elution fractions were measured by UV280 in a 96 well plate using a DropSense instrument prior to pooling. Pooled neutralized eluted antibody was sterile filtered into a 50 mL Falcon tube by 0.22 μm Millipore Steriflip using vacuum filtration system. The final concentrations were then similarly measured on the DropSense instrument by applying the specific extinction coefficient of each antibody.

As a polishing step, preparative size-exclusion chromatography was also performed (when necessary) to remove large amounts of aggregates to have monomer percentages greater than 95%. Briefly, HiLoad 26/600 Superdex200 preparative grade column was equilibrated with 600 mL of 60 mM sodium acetate pH 5.0 buffer by AKTA system. The Protein A purified antibody sample was loaded onto the column at a flow rate of 1.5 mL/min. Fractions (3 mL) were collected by the fraction collector after approximately one column volume or when the UV280 absorbance reached above the baseline. The fractions containing monomers determined by analytical size exclusion chromatography were pooled and sterile filtered into a 50 mL Falcon tube by 0.22 μm Millipore Steriflip using vacuum filtration system. The concentrations were measured similarly as mentioned before.

Analytical size exclusion chromatography

Purity was evaluated by analytical size exclusion chromatography using a 7.8 × 300 mm TSKgel G3000SWXL HPLC column (GE Healthcare) equilibrated with PBS containing 0.2 mol/L L-arginine (pH 6.8) with a flow rate of 0.5 mL/min PBS containing 0.2 mol/L L-arginine (pH 6.8) using an ACQUITY ultraperformance LC system (Waters, Milford, MA). The monomer and aggregate chromatogram peaks were identified and processed in reference to a molecular weight standard, and % monomer, % low and high molecular

weight species (%LMWS and %HMWS) were determined by calculating the area under the curve of the chromatograms using Empower software (Waters, Milford, MA; Table S1).

Non-specific binding measurements: ELISA #1

The non-specific binding measurements were performed using an ELISA method reported previously[9, 45] with some modifications. Immulon 2HB plates (3655TS, Thermo Fisher Scientific) were coated separately with six non-antigen reagents (Cardiolipin (50 μg/mL), keyhole limpet hemocyanin (5 μg/mL), lipopolysacchride (10 μg/mL), single and double stranded DNA (1 μg/mL) and insulin at 200 μg/mL) for 1 h at 37 °C. The plates were washed three times with 200 μL/well of PBS containing 0.05% Tween 20 (PBST) using a Biotek plate washer and were not blocked. Then 50 μL of each antibody of interest prepared at 1 μM in PBST was incubated in the wells for 1 h. The plates were washed three times with 200 μL/well of PBST before incubating with 50 μL of the secondary antibody at 10 ng/mL (HRP conjugated goat anti-human IgG antibody, 109–035-008, Jackson Immuno Research) for 1 h. The plates were developed with 50 μL of TMB substrate (TMBS-1000-01, Surmodics) after removal of any unbound secondary antibody with six washes in PBST. Color development was quenched with 50 μL of 2 M sulfuric acid after 5 min. Absorbance values were measured at 450 nm using a Biotek Synergy 2 plate reader. The signals obtained were normalized to adalimumab and bococizumab IgGs in each experiment as negative and positive controls, respectively. Normalized values were calculated as the absorbance for a given mAb minus the absorbance for adalimumab divided by the difference in absorbance for bococizumab and adalimumab.

Non-specific binding measurements: ELISA #2

The ELISA with baculovirus particles was performed similarly to previously reported method.[38] Briefly, the BVP stock (LakePharma) was first evaluated with reference antibodies to determine the optimal dilution to obtain best signal to noise readouts. Diluted BVP stock (1:100) in sodium carbonate buffer (pH 9.6) was determined to be the optimal dilution. Diluted BVP (50 μL per well) was incubated in Immulon 2HB plates at 4 °C overnight. Unbound particles were aspirated from the wells using Biotek plate washer. The plates were blocked with 200 μL of blocking buffer (PBS with 0.5% BSA) and incubated for 1 h before washing three times with 200 μL of PBS. 50 μL of each antibody, prepared at 1 μM in blocking buffer, was added to the wells and incubated for 1 h followed by six washes with 200 μL of PBS. Next, 50 μL of diluted secondary antibody at 10 ng/mL was added to the wells and incubated for 1 h followed by another six washes. Finally, 50 μL of TMB substrate was added to each well and incubated for 5 min. The reaction was quenched by adding 50 μL of 2 M sulfuric acid to each well. Absorbance values were measured at 450 nm using a Biotek Synergy 2 plate reader. Normalized values were calculated using the same method described for ELISA #1

Non-specific binding measurements: PolySpecificity (PSP) assay

The assay, including the preparation of soluble membrane protein and ovalbumin reagents, were performed as described in our previous work.[46] Briefly, non-specific binding measurements with soluble membrane proteins (PSP #1) and ovalbumin (PSP #2) were incubated with overnight antibody (15 μg/mL) coated Protein A magnetic beads (10002D,

Invitrogen). The reagent and bead complexes were incubated at 4 °C for 20 min for soluble membrane proteins, while ovalbumin was incubated 3 h at room temperature. The beads were then washed once and incubated with 0.001x streptavidin-AF647 (S32357, Invitrogen) and 0.001x goat anti-human Fc F(ab')2 AF-488 (H10120, Invitrogen) on ice for 4 min. As a final step, the beads were washed once more and resuspended in PBSB. The samples were analyzed for non-specific binding via flow cytometry to measure their median fluorescent intensities (MFI). Adalimumab and bococizumab (generated using the antibody variable regions from the clinical-stage antibodies on a common IgG1 framework) were analyzed in each experiment as negative (adalimumab) and positive (bococizumab) controls. Polyspecificity scores were calculated as the MFI for a given mAb minus the MFI for adalimumab divided by the difference in MFI values for bococizumab and adalimumab.

Diffusion interaction parameter (k_D) measurements

The antibody samples in acetate buffer were dialyzed into 10 mM histidine HCl (pH 6.0) buffer using 10 kD Slide-A-Lyzer dialysis cassettes (ThermoFisher Scientific) and concentrated to achieve greater than 12 mg/mL mAb. The concentrated sample variants were filtered using 0.2 micron filters before preparing them at six concentrations (10, 9, 7, 5, 2.5 and 1.25 mg/mL), transferred to 384-well plates (Greiner Bio-One) in duplicates, sealed with a film and centrifuged at 1200 rpm for 5 min. The apparent diffusion interaction parameters (k_D) were calculated from diffusion coefficients, as a function of antibody concentration, measured using the Wyatt DynaPro Plate Reader II dynamic light scattering instrument. The instrument was set up to measure diffusion coefficients 10 times and each measurement was performed for 5 s. The autocorrelation function was fit using the method of cumulants (Dynamics software, version 7.1) to measure mean diffusion coefficient values. The goodness of the fit was inspected, and any data points with a sum of squares (SOS) values greater than one were removed. The mean diffusion coefficients from triplicate experiments were plotted as a function of antibody concentration to obtain the diffusion interaction parameter values.

Homology Modeling

The fragment variable region (Fv) sequences were used to build homology models in an automated fashion using the Antibody Modeler feature in Molecular Operating Environment (MOE) Inc., 2019 by Chemical Computing group. The force field was set to Amber10: EHT with the internal and external dielectric values of 4 and 80, respectively. The non-bonded cutoff distances were set to 10 and 12 Å, and the Born solvation was used. Once the homology models were built, the C-termini of the heavy and light variable chains were capped by amidating to neutralize charges. The capped models were prepared for energy minimizations by using the structure preparation feature to remove any errors and protonate the models at pH 6.0 with 0.0001 M ionic strength or pH 7.4 with 0.15 M ionic strength. The prepared structures were subjected to energy minimization to root man square gradient (RMSG) below 0.00001 kcal/mol/Å^2.

Sequence and structure based molecular property calculations

The heavy and light chain sequences were used to calculate net charge of all 6 CDRs, V_L, V_H and Fv at pH 6 and pH 7.4 and also isoelectric points of Fv and IgG. The homology

models of Fv were used to calculate stability, charge and hydrophobic properties for the CDRs and Fv regions at both pH 6 and pH 7.4 using the property calculation feature in MOE 2019.

RESULTS

Design and production of clinical-stage antibody frameworks with HCDR3 sequence variation

Toward our goal of evaluating how CDR sequences impact antibody self-association and non-specific binding, we first chose four clinical-stage antibodies for analysis, namely lebrikizumab, siltuximab, trastuzumab and humanized OKT3 (hOKT3).[9, 44] These four antibodies have variable regions with a range of physicochemical properties and germlines (Table 1 and Fig. S1). The fragment variable (Fv) regions of the antibodies differ significantly in terms of their charges (−1.9 to +9.2 at pH 7.4) and isoelectric points (pIs of 5.4 to 9.3; Table 1). To generate additional diversity in heavy chain CDR3 (HCDR3) for the four antibodies, we selected a set of ten naturally occurring HCDR3s, each of which is ten residues long and differs in its physicochemical properties (Table 2). The ten different HCDR3s were grafted onto the V_H regions to generate a set of 42 IgG1 antibodies with diverse properties. This is less than the expected 44 antibodies because two of the HCDR3s (trastuzumab and hOKT3) were used for CDR grafting. Given that trastuzumab has an 11-residue HCDR3, the grafted trastuzumab variants have a tryptophan at the N-terminus of HCDR3 to keep the loop length constant (11 residues).

The antibodies were expressed as IgG1/kappa antibodies in mammalian cells and purified by Protein A. The quality of the purified variants was assessed by analytical size-exclusion chromatography (Table S1). Antibodies that were <90% monomer were further purified by size-exclusion chromatography. The purification yields were relatively high for the four scaffolds, including 29–124 mg/L for the lebrikizumab variants, 82–203 mg/L for the siltuximab variants, 99–151 mg/L for the trastuzumab variants and 24–187 mg/mL for the hOKT3 variants.

Antibody variants display trade-offs between specificity and colloidal stability

To evaluate potential trade-offs between different types of antibody colloidal interactions, we next evaluated non-specific binding at physiological conditions (pH 7.4, PBS) for the panel of antibody variants using two previously reported ELISAs and two forms a flow cytometry assay [PolySpecificity Particle (PSP) assay].[9, 38, 45, 46] First, we used an ELISA (referred to ELISA #1) for evaluating antibody non-specific interactions with six non-antigen reagents, namely cardiolipin, lipopolysaccharide (LPS), keyhole limpet hemocyanin (KLH), insulin, single and double stranded DNA (Fig. 2A). The parent antibodies (open circles in Fig. 2A) generally displayed relatively low levels of non-specific binding, although the higher pI parent antibodies (hOKT3 and trastuzumab) displayed modestly higher levels of non-specific binding relative to the lower pI antibodies (siltuximab and lebrikizumab). Interestingly, the grafted CDR variants generally displayed higher to much higher levels of non-specific binding than the parent antibodies. For the high pI antibodies (hOKT3 and trastuzumab), the positively charged HCDR3s (triangles) generally displayed higher levels

of non-specific binding than those with negatively charged HCDR3s (circles). For the lower pI antibodies (siltuximab and lebrikizumab), it is notable that the few antibody variants that display relatively highly levels of non-specific interactions have positively charged HCDR3s.

We also evaluated non-specific binding for the antibody panel using a second ELISA (referred to as ELISA #2) with immobilized baculovirus particles that present a range of proteins, glycans and lipids (Fig. 2B). Overall, the results were generally similar between the two ELISAs. The high pI antibody variants (hOKT3 and trastuzumab) displayed the highest levels of non-specific binding, while the lower pI antibodies (siltuximab and lebrikizumab) displayed the lowest levels of non-specific binding. Moreover, the effect of HCDR3 charge was less significant on the non-specific binding measurements by ELISA #2 than observed for ELISA #1 (Fig. 2A), although the trends were similar (Fig. 2A and 2B).

We next evaluated the antibody variants for their levels of non-specific interactions via a complementary flow cytometry-based assay, namely the PolySpecificity Particle (PSP) assay,[46] using two polyspecificity reagents (Fig. 2C–2D). These reagents included a complex mixture of soluble membrane proteins (SMP) isolated from CHO cells (Fig. 2C) and ovalbumin (OVA, Fig. 2D). Overall, the PSP assays revealed that OKT3 has the highest levels of non-specific binding, while most of the other antibody variants display low levels of non-specific binding. However, the siltuximab variants unexpectedly display a wide range of levels of non-specific binding to soluble membrane proteins, including levels that were similar to or higher than those for OKT3 (Fig. 2C).

Given the strong impact of Fv charge and HCDR3 sequence on antibody non-specific binding in physiological conditions (pH 7.4, PBS), we also evaluated the impact of these properties on antibody self-association in a standard formulation condition (pH 6.0, 10 mM histidine; Figs. 3 and S2). This formulation condition was chosen because it is a consensus pH and buffer system for mAb therapeutics,[10] and pH 6 is within the most common range of pHs (e.g., pH 5.5–6.2) of most approved antibody therapeutics since 2015.[47] We evaluated antibody self-association by measuring the diffusion interaction parameter (k_D), which is the slope of the mutual diffusion coefficient as a function of protein concentration. Values of k_D >−8.2 to −8.9 mL/g generally are linked to repulsive antibody self-interactions, while smaller (more negative) values are generally to attractive self-interactions.[21, 48] Interestingly, all antibody variants displayed repulsive self-interactions, as judged by their positive k_D values. Moreover, the high pI antibodies (hOKT3 and trastuzumab) displayed the most repulsive self-interactions. The hOKT3 grafted variants displayed reduced repulsion relative to the parental antibody regardless of the HCDR3 charge. Conversely, the antibodies with lower pIs (siltuximab and lebrikizumab) displayed weakly-to-moderately repulsive self-interactions, and the variants with the most repulsive self-interactions had positively charged HCDR3s (Fig. 3). We also observe similar k_D values for the four parental antibodies at pH 5.5 and 6.5 (Fig. S3), suggesting the general patterns of behavior are weakly impacted by pH in this range of pH values (pH 5.5–6.5) that are relevant to many mAb therapeutic formulations.[10]

To evaluate potential trade-offs between antibody non-specific binding in physiological conditions (PBS, pH 7.4) and self-association in a standard formulation condition (pH 6.0, 10 mM histidine), we plotted them against each other (Fig. 4). For reference, antibodies with k_D values >20 mL/g in standard formulation conditions (vertical dotted line in Fig. 4) are particularly desirable because they have been shown to have a low likelihood of viscous or opalescent behavior when formulated at high concentrations (>100 mg/mL) for subcutaneous delivery.[10] Likewise, antibodies with low levels of non-specific interactions, such as the levels for the prototypical antibody trastuzumab, are desirable to minimize off-target interactions *in vivo* that can lead to fast antibody clearance. For simplicity, the normalized value of trastuzumab non-specific interactions in each assay is indicated with a dotted horizontal line. Interestingly, most of the antibody variants either displayed both highly repulsive self-interactions and high levels of non-specific binding or both weakly repulsive self-interactions and low levels of non-specific binding. None of the antibody variants displayed as low of levels of non-specific binding as trastuzumab in all assays while displaying highly repulsive self-interactions (k_D >20 mL/g). The two types of colloidal interactions (self- and non-specific interactions) are thus positively correlated but with opposite implications (Fig. S4). ELISA #2 exhibits a stronger correlation with k_D (Spearman's ρ of 0.76) than observed for ELISA #1 (Spearman's ρ of 0.49). The correlations were weaker between k_D and the PSP assays [Spearman's ρ of 0.21 (PSP #1, SMP) and 0.48 (PSP #2, OVA)].

Molecular properties correlated with non-specific binding and colloidal stability

Given the strong apparent impact of Fv charge on both antibody self-interactions and non-specific binding, we next evaluated correlations for both biophysical measurements with Fv charge and IgG isoelectric point (Table 3). As expected, the correlations were strong (Spearman's ρ values of 0.75–0.89) and highly significant (p-values $<10^{-7}$).

We also evaluated correlations between antibody non-specific interactions and self-association for several other sequence- and structure-based antibody properties (Table 3). Many of the charge properties, calculated either based on sequence or structure, displayed strong positive correlations with non-specific interactions and self-association. Interestingly, CDR net charge was much more strongly correlated with the average measurements of the four non-specific binding assays (ρ of 0.69, p-value <0.0001) than with the measurements of self-interactions (ρ of 0.49, p-value of <0.05). Structure-based calculations revealed significant correlations between the average of the non-specific interactions assays and the total area of positively charged patches in the CDRs and Fv region (ρ of 0.75–0.82, p-values <0.00001).

The structure-based calculations also identified strong positive correlations between Fv hydrophilic surface area due to polar residues (including charged residues) and both non-specific and self-interactions (ρ of 0.52–0.6; Table 3). This is likely due to the dominant contributions of positively charged residues, which are included in the hydrophilic area calculations, to each of the biophysical properties. The calculations of hydrophobicity reveal weaker and more complex correlations, as hydrophobic surface and patch areas are negatively correlated with each property, while measures of the distribution of

hydrophobic residues (hydrophobic moment and imbalance) are positively correlated with these properties.

The dominant role of antibody charge in mediating both non-specific interactions and repulsive self-association suggests that there may be ranges of antibody isoelectric points that are best at balancing the competing demands of high antibody colloidal stability (high levels of repulsive self-interactions) in formulation conditions with the high antibody specificity (low levels of non-specific binding) in physiological conditions. Therefore, we plotted both biophysical properties against each other and highlighted ranges of Fv isoelectric points (Fig. 5). Notably, IgG1s with Fv isoelectric points between 7.5–9 displayed the best combinations of these properties, as seen for the average ELISA (Fig. 5A) and PSP (Fig. 5B) measurements. In particular, the antibodies in these groups generally displayed strongly repulsive self-interactions with low-to-moderate levels of non-specific interactions. Conversely, antibodies with higher isoelectric points displayed high levels of non-specific interactions, while those with lower isoelectric points displayed weaker repulsive self-interactions. Interestingly, the Fv regions from most (61%) of 79 approved antibody drugs have isoelectric points between 7.5–9, suggesting this range of antibody charge properties may be particularly attractive for therapeutic development (Fig. 6A). Human antibody repertoires (14037 mAbs[49, 50]) display similar but slightly higher Fv isoelectric points, as only 49% of such antibodies have isoelectric points between 7.5–9 (Fig. 6B). This may reveal a modest bias toward Fv isoelectric points with intermediate values of 7.5–9 during therapeutic antibody development, although the differences between the two distributions are not statistically significant.

DISCUSSION

Our studies demonstrate natural trade-offs between two key molecular properties of antibody therapeutics, namely non-specific binding in physiological conditions (pH 7.4, PBS) and self-association in a standard formulation condition (pH 6, 10 mM histidine). Moreover, we demonstrate for the first time, at least to our knowledge, that intermediate ranges of antibody isoelectric point (Fv pIs of 7.5–9, corresponding to IgG1 pIs of 8–8.5) are best for balancing the competing requirements of high colloidal stability in formulation conditions and low non-specific binding in physiological conditions.

While it is obvious that such simple rules of thumb will fail in cases where non-electrostatic interactions play a key role in either type of biophysical property [e.g., see[51] for examples of mutations that cannot be entirely explained by these rules of thumb], it is interesting that this finding is generally consistent with a surprisingly large number of previous observations. For example, several studies have evaluated the self-association behavior of antibody variants in formulation conditions that are either the same or similar to those studied in this work (pH 5–6 and low ionic strength).[10, 20, 26] One notable example, namely omalizumab, displays abnormally high viscosity when concentrated to >100 mg/mL (pH 6, histidine, 15 mM ionic strength), and it has a theoretical Fv pI of 5.8.[20] Notably, introducing mutations into the CDRs that increases the Fv pI to 7.9 significantly reduces self-association and viscosity, which is consistent with our finding that antibodies display highly repulsive self-interactions at Fv pIs between 7.5–9.

More generally, a recent study demonstrated that antibodies with IgG isoelectric points >8 typically displayed favorable viscoelastic and opalescent behavior when concentrated to 150 mg/mL in the same formulation condition evaluated in this work,[10] which is also consistent with our findings that IgG1s with pIs in the range of 8–8.5 display repulsive self-interactions. Our findings also agree with several other studies that high pI antibodies typically display strongly repulsive self-interactions and/or low viscosities, and low pI antibodies typically display stronger self-association and/or increased viscosity in standard formulation conditions.[21–23, 26, 28, 42, 51, 52] Finally, it is important to note that increasing the ionic strength in weakly basic formulations (e.g., pH 6) will, in some cases, reduce antibody self-association,[18, 20, 53, 54] and should be investigated further in the future in relation to our findings.

Our findings are also consistent with several other studies on the molecular determinants of antibody non-specific interactions in physiological conditions. For example, several studies report that increased positive charge in the CDRs or Fv in general promotes antibody non-specific binding,[14, 35, 55–59] as we observed for high pI antibodies in this work. One of the most striking examples of this is the cationization of polyclonal IgGs using chemical derivatization, which shifts the pI of the IgG antibody mixture from a pI range of 5.9–9 to 8.7–10.3, and increases non-specific cellular uptake several fold.[59] Conversely, multiple studies report that increased negative charge in the CDRs or Fv in general are linked to reduced non-specific binding.[35, 60, 61] Moreover, we evaluated three sets of previously reported non-specific binding data for clinical-stage antibodies[9] and found that antibodies with Fv pIs ≥8.7 display significantly higher levels of non-specific binding than antibodies with lower Fv pIs (*p*-values of 0.0001-0.01 for 2×2 contingency table analysis), which is also consistent with our findings in this study.

It also notable that reducing IgG pI has been reported to reduce antibody clearance *in vivo*,[31, 33, 37, 62] which is likely due to reduced non-specific interactions along with other contributing factors. Notably, a previous study predicted that Fv charge <+6.2 (and >0) at pH 5.5 was optimal for promoting favorable antibody pharmacokinetics.[42] This range of Fv charges corresponds to antibodies with Fv pIs of 4.9–8.7, which is consistent with our rule of thumb that antibodies with Fv pIs <9 have low-to-moderate levels of non-specific interactions.

Our findings motivate the development of phenomenological models, rather than overly simple rules of thumb, that can better predict antibodies with Fv properties that balance the competing demands of low self-association in formulation conditions and low non-specific binding in physiological conditions. This will require much larger and more diverse datasets, including those with antibody framework and CDR diversity. Additionally, in this study we only focus on the human IgG1 subclass because it represents the largest proportion (~two thirds) of the approved antibody therapeutics. Future work will be required to further expand our analysis to other subclasses such as IgG2 and IgG4 to test the generality of our findings. To enable the generation of such large datasets, it will be critical to use methods that can evaluate antibody non-specific and self-interactions at ultra-dilute concentrations (~0.001–0.01 mg/mL). Two assays that are particularly well suited for this challenge are the PSP assay, which was used this study, for measuring non-specific interactions in physiological

conditions and the CS-SINS assay,[63] a refined version of AC-SINS[64–66] that was reported after this study was completed, for measuring self-interactions in standard formulation conditions (pH 6 and 10 mm histidine). The combination of these two assays holds great potential for generating large datasets (hundreds to thousands of mAbs) for developing models that can predict both antibody non-specific and self-interactions, which we believe are critical to advance the identification of therapeutic antibodies with drug-like colloidal properties and increased likelihood of success in clinical development.

In conclusion, our studies resolve some existing conflicts in the field that report seemingly contradictory findings as to whether low or high pI antibodies have optimal physicochemical properties for antibody development. The fact that neither extreme is desired naturally leads to the conclusion that intermediate pI antibodies are generally best at balancing the competing demands of antibody colloidal properties in formulation and physiological conditions. It will be important in the future to identify more refined predictors of antibodies with the best combinations of *in vitro* (formulation) and *in vivo* (bioavailability) properties, which will require accounting for other types of charge (e.g., dipole-dipole) and non-charged (e.g., hydrophobic) interactions. These modelling efforts hold great potential for improving antibody candidate selection and protein engineering at early stages of drug development to reduce the risk for problems that may emerge later in drug development and clinical trials.

Supplementary Material

Refer to Web version on PubMed Central for supplementary material.

ACKNOWLEDGEMENTS

We thank members of the Tessier lab for their helpful suggestions. We also thank members of the downstream processing group at Biotherapeutics Discovery department of Boehringer Ingelheim Pharmaceuticals for providing help with second step purification of antibodies. This work was supported and funded by the Boehringer Ingelheim Pharmaceuticals Inc., Ridgefield, Connecticut, the National Institutes of Health (R35GM136300 to P.M.T.), and the Albert M. Mattocks Chair (to P.M.T).

SUPPORTING INFORMATION

The supporting figures include: i) a summary of the antibody amino acid sequences used in this study, measurements of diffusion interaction parameters (k_D) for all of variants at pH 6 (10 mM histidine) and for a subset of the parent mAbs at pH 5.5–6.5 (10 mM histidine); and ii) a comparison of colloidal interactions in physiological (PBS, pH 7.4) and formulation (10 mM histidine, pH 6) conditions. The supporting tables include: i) monomer quality assessment by analytical size exclusion chromatography; and ii) thermal melting temperature (midpoint of unfolding) of the purified antibody variants.

REFERENCES

1. Biswas NR; Das GK; Dubey AK, Monoclonal antibodies in ophthalmology. Nepal Med Coll J 2010, 12 (4), 264–71. [PubMed: 21744772]
2. Buss NA; Henderson SJ; McFarlane M; Shenton JM; de Haan L, Monoclonal antibody therapeutics: history and future. Curr Opin Pharmacol 2012, 12 (5), 615–22. [PubMed: 22920732]
3. Hafeez U; Gan HK; Scott AM, Monoclonal antibodies as immunomodulatory therapy against cancer and autoimmune diseases. Curr Opin Pharmacol 2018, 41, 114–121. [PubMed: 29883853]
4. Matera MG; Page C; Rogliani P; Calzetta L; Cazzola M, Therapeutic Monoclonal Antibodies for the Treatment of Chronic Obstructive Pulmonary Disease. Drugs 2016, 76 (13), 1257–1270. [PubMed: 27506851]

5. Singh S; Kumar NK; Dwiwedi P; Charan J; Kaur R; Sidhu P; Chugh VK, Monoclonal Antibodies: A Review. Curr Clin Pharmacol 2018, 13 (2), 85–99. [PubMed: 28799485]

6. Kaplon H; Muralidharan M; Schneider Z; Reichert JM, Antibodies to watch in 2020. MAbs 2020, 12 (1), 1703531. [PubMed: 31847708]

7. Carter PJ, Potent antibody therapeutics by design. Nat Rev Immunol 2006, 6 (5), 343–57. [PubMed: 16622479]

8. Tiller KE; Tessier PM, Advances in Antibody Design. Annu Rev Biomed Eng 2015, 17, 191–216. [PubMed: 26274600]

9. Jain T; Sun T; Durand S; Hall A; Houston NR; Nett JH; Sharkey B; Bobrowicz B; Caffry I; Yu Y; Cao Y; Lynaugh H; Brown M; Baruah H; Gray LT; Krauland EM; Xu Y; Vasquez M; Wittrup KD, Biophysical properties of the clinical-stage antibody landscape. Proc Natl Acad Sci U S A 2017, 114 (5), 944–949. [PubMed: 28096333]

10. Kingsbury JS; Saini A; Auclair SM; Fu L; Lantz MM; Halloran KT; Calero-Rubio C; Schwenger W; Airiau CY; Zhang J; Gokarn YR, A single molecular descriptor to predict solution behavior of therapeutic antibodies. Sci Adv 2020, 6 (32), eabb0372.

11. Challa DK; Velmurugan R; Ober RJ; Sally Ward E, FcRn: from molecular interactions to regulation of IgG pharmacokinetics and functions. Curr Top Microbiol Immunol 2014, 382, 249–72. [PubMed: 25116104]

12. Ward ES; Zhou J; Ghetie V; Ober RJ, Evidence to support the cellular mechanism involved in serum IgG homeostasis in humans. Int Immunol 2003, 15 (2), 187–95. [PubMed: 12578848]

13. Sigounas G; Harindranath N; Donadel G; Notkins AL, Half-life of polyreactive antibodies. J Clin Immunol 1994, 14 (2), 134–40. [PubMed: 8195315]

14. Datta-Mannan A; Lu J; Witcher DR; Leung D; Tang Y; Wroblewski VJ, The interplay of non-specific binding, target-mediated clearance and FcRn interactions on the pharmacokinetics of humanized antibodies. MAbs 2015, 7 (6), 1084–93. [PubMed: 26337808]

15. Bumbaca D; Wong A; Drake E; Reyes AE 2nd; Lin BC; Stephan JP; Desnoyers L; Shen BQ; Dennis MS, Highly specific off-target binding identified and eliminated during the humanization of an antibody against FGF receptor 4. MAbs 2011, 3 (4), 376–86. [PubMed: 21540647]

16. Tabrizi MA; Tseng CM; Roskos LK, Elimination mechanisms of therapeutic monoclonal antibodies. Drug Discov Today 2006, 11 (1–2), 81–8. [PubMed: 16478695]

17. Bumbaca D; Boswell CA; Fielder PJ; Khawli LA, Physiochemical and biochemical factors influencing the pharmacokinetics of antibody therapeutics. AAPS J 2012, 14 (3), 554–8. [PubMed: 22610647]

18. Yadav S; Liu J; Shire SJ; Kalonia DS, Specific interactions in high concentration antibody solutions resulting in high viscosity. J Pharm Sci 2010, 99 (3), 1152–68. [PubMed: 19705420]

19. Yadav S; Shire SJ; Kalonia DS, Factors affecting the viscosity in high concentration solutions of different monoclonal antibodies. J Pharm Sci 2010, 99 (12), 4812–29. [PubMed: 20821382]

20. Yadav S; Sreedhara A; Kanai S; Liu J; Lien S; Lowman H; Kalonia DS; Shire SJ, Establishing a link between amino acid sequences and self-associating and viscoelastic behavior of two closely related monoclonal antibodies. Pharm Res 2011, 28 (7), 1750–64. [PubMed: 21626060]

21. Connolly BD; Petry C; Yadav S; Demeule B; Ciaccio N; Moore JM; Shire SJ; Gokarn YR, Weak interactions govern the viscosity of concentrated antibody solutions: high-throughput analysis using the diffusion interaction parameter. Biophys J 2012, 103 (1), 69–78. [PubMed: 22828333]

22. Yadav S; Laue TM; Kalonia DS; Singh SN; Shire SJ, The influence of charge distribution on self-association and viscosity behavior of monoclonal antibody solutions. Mol Pharm 2012, 9 (4), 791–802. [PubMed: 22352470]

23. Yadav S; Shire SJ; Kalonia DS, Viscosity behavior of high-concentration monoclonal antibody solutions: correlation with interaction parameter and electroviscous effects. J Pharm Sci 2012, 101 (3), 998–1011. [PubMed: 22113861]

24. Chaudhri A; Zarraga IE; Yadav S; Patapoff TW; Shire SJ; Voth GA, The role of amino acid sequence in the self-association of therapeutic monoclonal antibodies: insights from coarse-grained modeling. J Phys Chem B 2013, 117 (5), 1269–79. [PubMed: 23316912]

25. Neergaard MS; Kalonia DS; Parshad H; Nielsen AD; Moller EH; van de Weert M, Viscosity of high concentration protein formulations of monoclonal antibodies of the IgG1 and IgG4 subclass

- prediction of viscosity through protein-protein interaction measurements. Eur J Pharm Sci 2013, 49 (3), 400–10. [PubMed: 23624326]

26. Li L; Kumar S; Buck PM; Burns C; Lavoie J; Singh SK; Warne NW; Nichols P; Luksha N; Boardman D, Concentration dependent viscosity of monoclonal antibody solutions: explaining experimental behavior in terms of molecular properties. Pharm Res 2014, 31 (11), 3161–78. [PubMed: 24906598]
27. Pindrus M; Shire SJ; Kelley RF; Demeule B; Wong R; Xu Y; Yadav S, Solubility Challenges in High Concentration Monoclonal Antibody Formulations: Relationship with Amino Acid Sequence and Intermolecular Interactions. Mol Pharm 2015, 12 (11), 3896–907. [PubMed: 26407030]
28. Nichols P; Li L; Kumar S; Buck PM; Singh SK; Goswami S; Balthazor B; Conley TR; Sek D; Allen MJ, Rational design of viscosity reducing mutants of a monoclonal antibody: hydrophobic versus electrostatic inter-molecular interactions. MAbs 2015, 7 (1), 212–30. [PubMed: 25559441]
29. Kumar S; Roffi K; Tomar DS; Cirelli D; Luksha N; Meyer D; Mitchell J; Allen MJ; Li L, Rational optimization of a monoclonal antibody for simultaneous improvements in its solution properties and biological activity. Protein Eng Des Sel 2018, 31 (7–8), 313–325. [PubMed: 30189027]
30. Matsuoka T; Miyauchi R; Nagaoka N; Hasegawa J, Mitigation of liquid-liquid phase separation of a monoclonal antibody by mutations of negative charges on the Fab surface. PLoS One 2020, 15 (10), e0240673. [PubMed: 33125371]
31. Bumbaca Yadav D; Sharma VK; Boswell CA; Hotzel I; Tesar D; Shang Y; Ying Y; Fischer SK; Grogan JL; Chiang EY; Urban K; Ulufatu S; Khawli LA; Prabhu S; Joseph S; Kelley RF, Evaluating the Use of Antibody Variable Region (Fv) Charge as a Risk Assessment Tool for Predicting Typical Cynomolgus Monkey Pharmacokinetics. J Biol Chem 2015, 290 (50), 29732–41. [PubMed: 26491012]
32. Datta-Mannan A; Thangaraju A; Leung D; Tang Y; Witcher DR; Lu J; Wroblewski VJ, Balancing charge in the complementarity-determining regions of humanized mAbs without affecting pI reduces non-specific binding and improves the pharmacokinetics. MAbs 2015, 7 (3), 483–93. [PubMed: 25695748]
33. Li B; Tesar D; Boswell CA; Cahaya HS; Wong A; Zhang J; Meng YG; Eigenbrot C; Pantua H; Diao J; Kapadia SB; Deng R; Kelley RF, Framework selection can influence pharmacokinetics of a humanized therapeutic antibody through differences in molecule charge. MAbs 2014, 6 (5), 1255–64. [PubMed: 25517310]
34. Piche-Nicholas NM; Avery LB; King AC; Kavosi M; Wang M; O'Hara DM; Tchistiakova L; Katragadda M, Changes in complementarity-determining regions significantly alter IgG binding to the neonatal Fc receptor (FcRn) and pharmacokinetics. MAbs 2018, 10 (1), 81–94. [PubMed: 28991504]
35. Rabia LA; Zhang Y; Ludwig SD; Julian MC; Tessier PM, Net charge of antibody complementarity-determining regions is a key predictor of specificity. Protein Eng Des Sel 2018, 31 (11), 409–418. [PubMed: 30770934]
36. Avery LB; Wade J; Wang M; Tam A; King A; Piche-Nicholas N; Kavosi MS; Penn S; Cirelli D; Kurz JC; Zhang M; Cunningham O; Jones R; Fennell BJ; McDonnell B; Sakorafas P; Apgar J; Finlay WJ; Lin L; Bloom L; O'Hara DM, Establishing in vitro in vivo correlations to screen monoclonal antibodies for physicochemical properties related to favorable human pharmacokinetics. MAbs 2018, 10 (2), 244–255. [PubMed: 29271699]
37. Igawa T; Tsunoda H; Tachibana T; Maeda A; Mimoto F; Moriyama C; Nanami M; Sekimori Y; Nabuchi Y; Aso Y; Hattori K, Reduced elimination of IgG antibodies by engineering the variable region. Protein Eng Des Sel 2010, 23 (5), 385–92. [PubMed: 20159773]
38. Hotzel I; Theil FP; Bernstein LJ; Prabhu S; Deng R; Quintana L; Lutman J; Sibia R; Chan P; Bumbaca D; Fielder P; Carter PJ; Kelley RF, A strategy for risk mitigation of antibodies with fast clearance. MAbs 2012, 4 (6), 753–60. [PubMed: 23778268]
39. Crowell SR; Wang K; Famili A; Shatz W; Loyet KM; Chang V; Liu Y; Prabhu S; Kamath AV; Kelley RF, Influence of Charge, Hydrophobicity, and Size on Vitreous Pharmacokinetics of Large Molecules. Transl Vis Sci Technol 2019, 8 (6), 1.
40. Datta-Mannan A; Estwick S; Zhou C; Choi H; Douglass NE; Witcher DR; Lu J; Beidler C; Millican R, Influence of physiochemical properties on the subcutaneous absorption and bioavailability of monoclonal antibodies. MAbs 2020, 12 (1), 1770028. [PubMed: 32486889]

41. Singh SN; Yadav S; Shire SJ; Kalonia DS, Dipole-dipole interaction in antibody solutions: correlation with viscosity behavior at high concentration. Pharm Res 2014, 31 (9), 2549–58. [PubMed: 24639233]
42. Sharma VK; Patapoff TW; Kabakoff B; Pai S; Hilario E; Zhang B; Li C; Borisov O; Kelley RF; Chorny I; Zhou JZ; Dill KA; Swartz TE, In silico selection of therapeutic antibodies for development: viscosity, clearance, and chemical stability. Proc Natl Acad Sci U S A 2014, 111 (52), 18601–6. [PubMed: 25512516]
43. Dobson CL; Devine PW; Phillips JJ; Higazi DR; Lloyd C; Popovic B; Arnold J; Buchanan A; Lewis A; Goodman J; van der Walle CF; Thornton P; Vinall L; Lowne D; Aagaard A; Olsson LL; Ridderstad Wollberg A; Welsh F; Karamanos TK; Pashley CL; Iadanza MG; Ranson NA; Ashcroft AE; Kippen AD; Vaughan TJ; Radford SE; Lowe DC, Engineering the surface properties of a human monoclonal antibody prevents self-association and rapid clearance in vivo. Sci Rep 2016, 6, 38644. [PubMed: 27995962]
44. Ellis Ronald IL; Tal Michael IL; Samira Sarit IL; Rachamim Nurit IL; Jones Timothy David GB; Carr Francis Joseph GB; Dotan Shahar IL ANTICORPS HUMANISÉS POUR LE GROUPE DE DIFFÉRENTIATION 3 (CD3) | HUMANIZED ANTIBODIES TO CLUSTER OF DIFFERENTIATION 3 (CD3) WO2013186613A1, 2013.
45. Mouquet H; Scheid JF; Zoller MJ; Krogsgaard M; Ott RG; Shukair S; Artyomov MN; Pietzsch J; Connors M; Pereyra F; Walker BD; Ho DD; Wilson PC; Seaman MS; Eisen HN; Chakraborty AK; Hope TJ; Ravetch JV; Wardemann H; Nussenzweig MC, Polyreactivity increases the apparent affinity of anti-HIV antibodies by heteroligation. Nature 2010, 467 (7315), 591–5. [PubMed: 20882016]
46. Makowski EK; Wu L; Desai AA; Tessier PM, Highly sensitive detection of antibody nonspecific interactions using flow cytometry. MAbs 2021, 13 (1), 1951426. [PubMed: 34313552]
47. Strickley RG; Lambert WJ, A review of Formulations of Commercially Available Antibodies. J Pharm Sci 2021, 110 (7), 2590–2608 e56. [PubMed: 33789155]
48. Lehermayr C; Mahler HC; Mader K; Fischer S, Assessment of net charge and protein-protein interactions of different monoclonal antibodies. J Pharm Sci 2011, 100 (7), 2551–62. [PubMed: 21294130]
49. Krawczyk K; Raybould MIJ; Kovaltsuk A; Deane CM, Looking for therapeutic antibodies in next-generation sequencing repositories. MAbs 2019, 11 (7), 1197–1205. [PubMed: 31216939]
50. Raybould MIJ; Marks C; Krawczyk K; Taddese B; Nowak J; Lewis AP; Bujotzek A; Shi J; Deane CM, Five computational developability guidelines for therapeutic antibody profiling. Proc Natl Acad Sci U S A 2019, 116 (10), 4025–4030. [PubMed: 30765520]
51. Apgar JR; Tam ASP; Sorm R; Moesta S; King AC; Yang H; Kelleher K; Murphy D; D'Antona AM; Yan G; Zhong X; Rodriguez L; Ma W; Ferguson DE; Carven GJ; Bennett EM; Lin L, Modeling and mitigation of high-concentration antibody viscosity through structure-based computer-aided protein design. PLoS One 2020, 15 (5), e0232713. [PubMed: 32379792]
52. Arora J; Hu Y; Esfandiary R; Sathish HA; Bishop SM; Joshi SB; Middaugh CR; Volkin DB; Weis DD, Charge-mediated Fab-Fc interactions in an IgG1 antibody induce reversible self-association, cluster formation, and elevated viscosity. MAbs 2016, 8 (8), 1561–1574. [PubMed: 27560842]
53. Kanai S; Liu J; Patapoff TW; Shire SJ, Reversible self-association of a concentrated monoclonal antibody solution mediated by Fab-Fab interaction that impacts solution viscosity. J Pharm Sci 2008, 97 (10), 4219–27. [PubMed: 18240303]
54. Liu J; Nguyen MD; Andya JD; Shire SJ, Reversible self-association increases the viscosity of a concentrated monoclonal antibody in aqueous solution. J Pharm Sci 2005, 94 (9), 1928–40. [PubMed: 16052543]
55. Wardemann H; Yurasov S; Schaefer A; Young JW; Meffre E; Nussenzweig MC, Predominant autoantibody production by early human B cell precursors. Science 2003, 301 (5638), 1374–7. [PubMed: 12920303]
56. Tiller KE; Li L; Kumar S; Julian MC; Garde S; Tessier PM, Arginine mutations in antibody complementarity-determining regions display context-dependent affinity/specificity trade-offs. J Biol Chem 2017, 292 (40), 16638–16652. [PubMed: 28778924]

57. Birtalan S; Zhang Y; Fellouse FA; Shao L; Schaefer G; Sidhu SS, The intrinsic contributions of tyrosine, serine, glycine and arginine to the affinity and specificity of antibodies. J Mol Biol 2008, 377 (5), 1518–28. [PubMed: 18336836]
58. Birtalan S; Fisher RD; Sidhu SS, The functional capacity of the natural amino acids for molecular recognition. Mol Biosyst 2010, 6 (7), 1186–94. [PubMed: 20383388]
59. Hong G; Chappey O; Niel E; Scherrmann JM, Enhanced cellular uptake and transport of polyclonal immunoglobulin G and fab after their cationization. J Drug Target 2000, 8 (2), 67–77. [PubMed: 10852339]
60. Zhang Y; Wu L; Gupta P; Desai AA; Smith MD; Rabia LA; Ludwig SD; Tessier PM, Physicochemical Rules for Identifying Monoclonal Antibodies with Drug-like Specificity. Mol Pharm 2020, 17 (7), 2555–2569. [PubMed: 32453957]
61. Sakhnini LI; Greisen PJ; Wiberg C; Bozoky Z; Lund S; Wolf Perez AM; Karkov HS; Huus K; Hansen JJ; Bulow L; Lorenzen N; Dainiak MB; Pedersen AK, Improving the Developability of an Antigen Binding Fragment by Aspartate Substitutions. Biochemistry 2019, 58 (24), 2750–2759. [PubMed: 31117388]
62. Boswell CA; Tesar DB; Mukhyala K; Theil FP; Fielder PJ; Khawli LA, Effects of charge on antibody tissue distribution and pharmacokinetics. Bioconjug Chem 2010, 21 (12), 2153–63. [PubMed: 21053952]
63. Starr CG; Makowski EK; Wu L; Berg B; Kingsbury JS; Gokarn YR; Tessier PM, Ultradilute Measurements of Self-Association for the Identification of Antibodies with Favorable High-Concentration Solution Properties. Mol Pharm 2021, 18 (7), 2744–2753. [PubMed: 34105965]
64. Wu J; Schultz JS; Weldon CL; Sule SV; Chai Q; Geng SB; Dickinson CD; Tessier PM, Discovery of highly soluble antibodies prior to purification using affinity-capture self-interaction nanoparticle spectroscopy. Protein Eng Des Sel 2015, 28 (10), 403–14. [PubMed: 26363633]
65. Geng SB; Wu J; Alam ME; Schultz JS; Dickinson CD; Seminer CR; Tessier PM, Facile Preparation of Stable Antibody-Gold Conjugates and Application to Affinity-Capture Self-Interaction Nanoparticle Spectroscopy. Bioconjug Chem 2016, 27 (10), 2287–2300. [PubMed: 27494306]
66. Alam ME; Geng SB; Bender C; Ludwig SD; Linden L; Hoet R; Tessier PM, Biophysical and Sequence-Based Methods for Identifying Monovalent and Bivalent Antibodies with High Colloidal Stability. Mol Pharm 2018, 15 (1), 150–163. [PubMed: 29154550]
67. Greene E; Cazacu D; Tamot N; Castellano S; Datar A; Kronkaitis A; Gebhard D; Reed J; Mawson P; Florin L; Rossi N; Lauer A; Juckem L; Nixon A; Wenger T; Sen S, Optimization of a transient antibody expression platform towards high titer and efficiency. Biotechnol J 2020, e2000251.

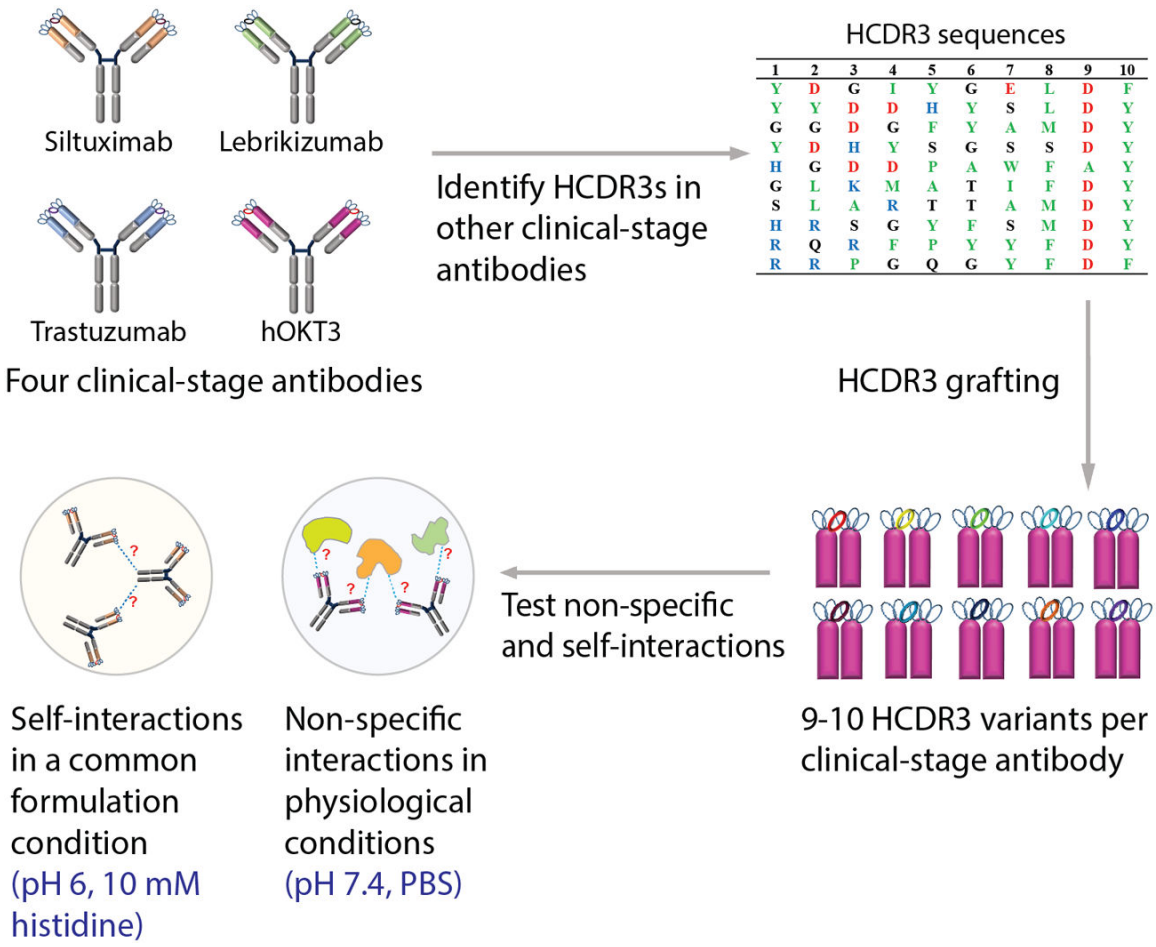

Figure 1. Design of a panel of antibody variants based on four clinical-stage antibodies with grafted heavy chain CDR3s.

Antibody variants were designed using the variable regions of four clinical-stage antibodies, namely humanized OKT3 (hOKT3), trastuzumab, siltuximab and lebrikizumab, that were grafted onto a common IgG1 scaffold. The heavy chain CDR3 (HCDR3) loops from ten clinical-stage antibodies (carlumab, muromonab, trastuzumab, bapineuzumab, farletuzumab, seribantumab, tocilizumab, girentuximab, lenzilumab and ustekinumab) were grafted onto each of the four clinical-stage antibody scaffolds. The panel of grafted antibodies was evaluated in terms of antibody self-association in a standard formulation condition (pH 6, 10 mM histidine) and physiological conditions (pH 7.4, PBS) to evaluate potential trade-offs between these two properties. The muromonab HCDR3 contains a cysteine residue that was mutated to serine in this study.

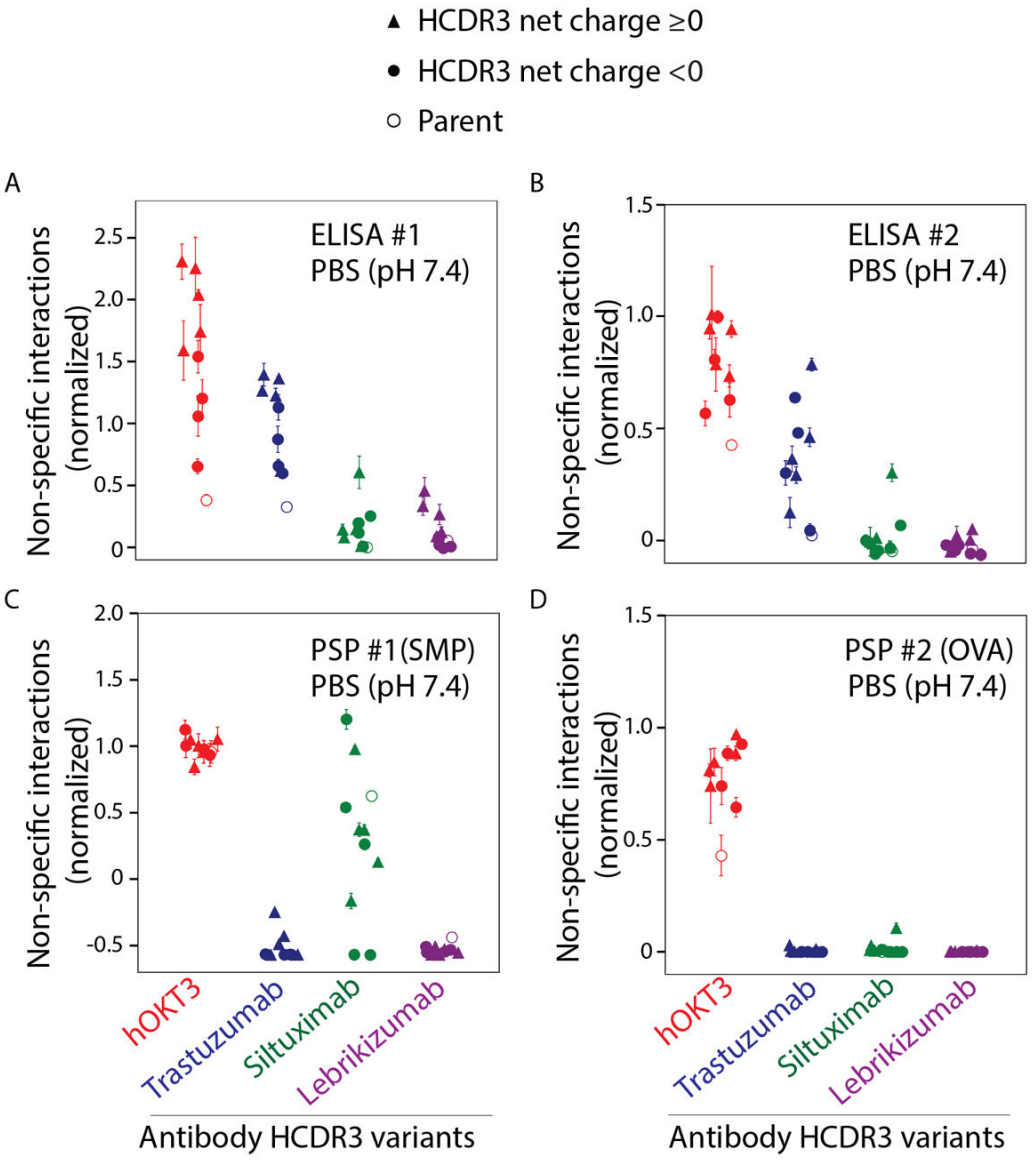

Figure 2. Evaluation of non-specific interactions for grafted antibody variants in physiological conditions (pH 7.4, PBS).

The antibody variants were evaluated using two ELISAs (#1 and #2), one with (A) with six different reagents (cardiolipin, LPS, KLH, ssDNA, dsDNA and insulin) and the second assay with (B) baculovirus particles (BVP). The variants were also evaluated using two flow cytometry (Polyspecificity Particle, PSP) assays, one with (C) soluble membrane proteins (SMP, PSP #1) and second one with (D) ovalbumin (OVA, PSP#2). ELISA and PSP assay values were normalized on a scale of 0 to 1 using adalimumab and bococizumab as negative and positive controls for nonspecific binding, respectively. The parental antibodies are indicated in open circles, while the negatively charged HCDR3s are indicated in filled circles and the positively charged HCDR3s are indicated in filled triangles. The values reported are averages for three independent experiments, and the error bars are standard deviations.

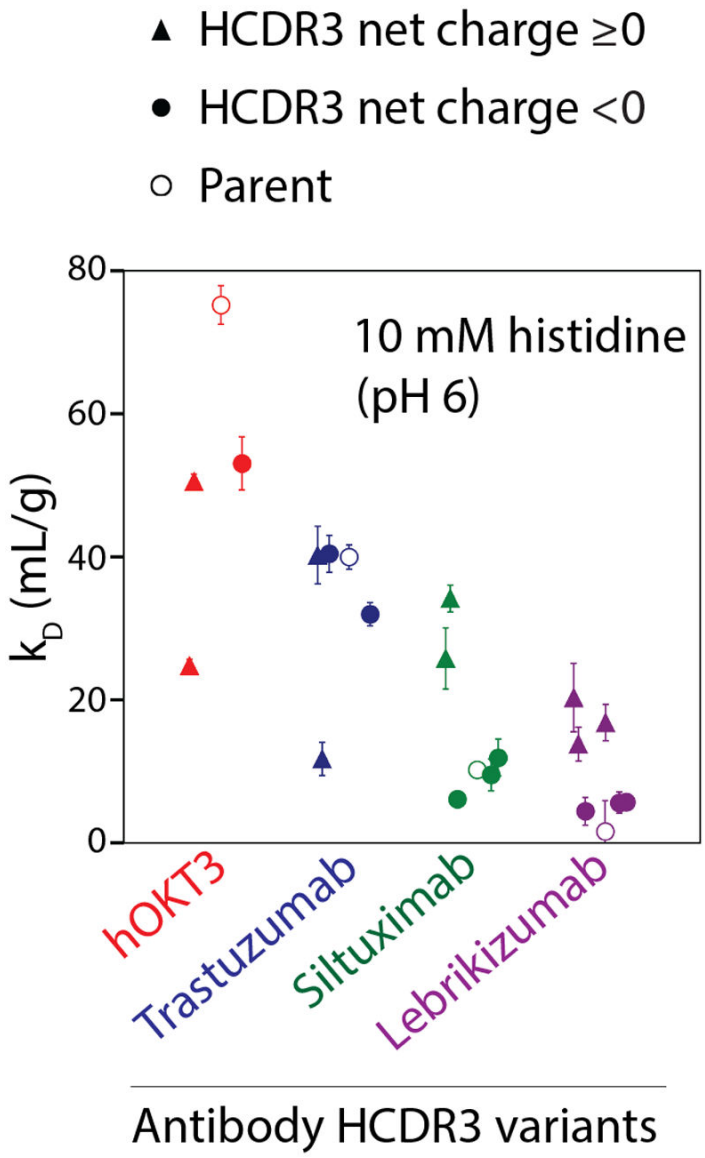

Figure 3. Evaluation of self-interactions for grafted antibody variants in a standard formulation condition (pH 6, 10 mM histidine).

The antibody variants were evaluated using dynamic light scattering to measure diffusion interaction parameters (k_D). The parental antibodies are indicated in open circles, while the negatively charged HCDRs are indicated in filled circles and the positively charged HCDR3s are indicated in filled triangles. The values reported are averages for three independent experiments, and the error bars are standard deviations.

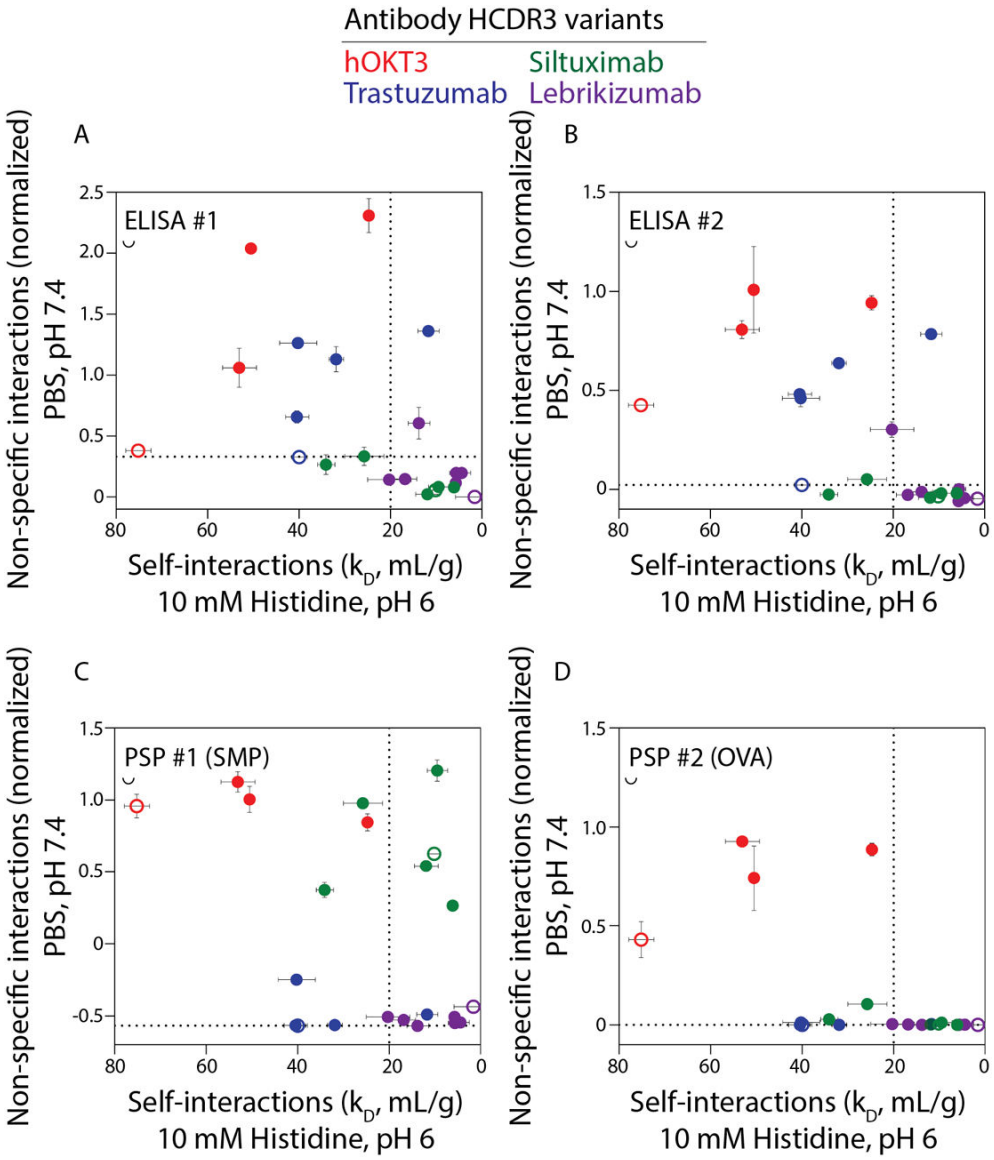

Figure 4. Trade-offs between antibody non-specific interactions in physiological conditions and self-interactions in a standard formulation condition.

Comparison of antibody self-interactions (k_D, diffusion interaction parameter) and nonspecific binding using (A) ELISA #1, (B) ELISA #2, (C) PSP #1 and (D) PSP #2. The dotted line at a k_D value of 20 mL/g indicates a previously reported threshold for strongly repulsive self-interactions corresponding to desirable viscoelastic and opalescent properties for concentrated antibody formulations.[10] The dotted line is the normalized non-specific binding value for trastuzumab, which is used as a threshold for low levels of non-specific binding in each assay. The parental antibodies are indicated in open circles. Notably, antibodies with low non-specific binding generally also display low levels of repulsive self-interactions (small k_D values). Conversely, antibodies that generally display highly repulsive self-interactions (large k_D values) also generally display high levels of non-specific binding.

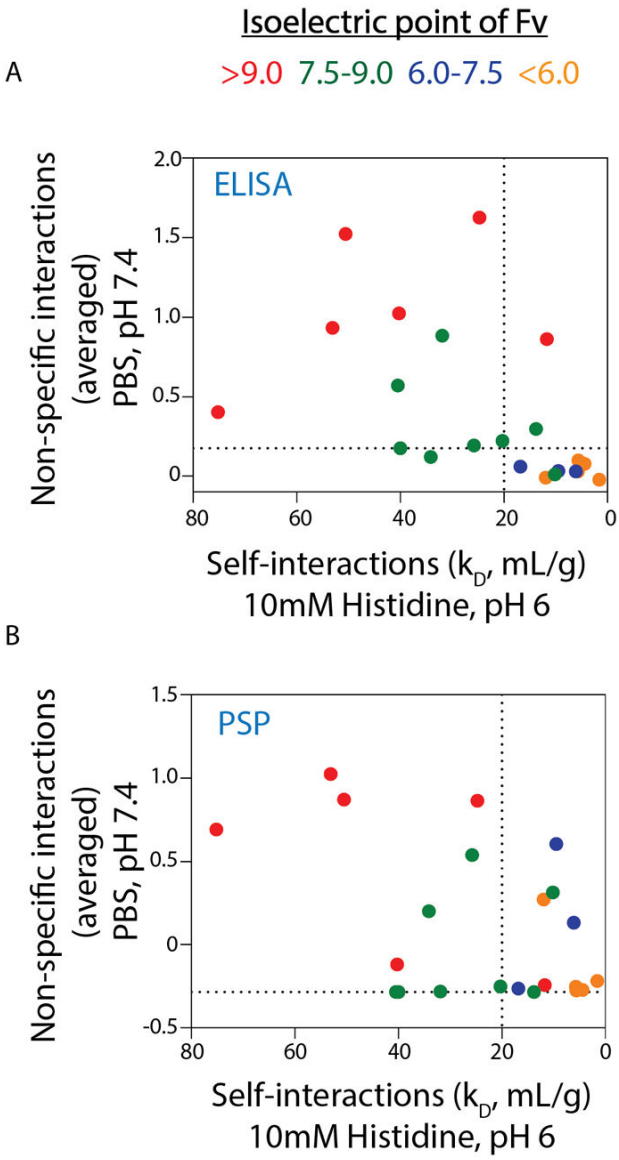

Figure 5. Antibodies with intermediate Fv isoelectric points display the best combination of formulation and physiological colloidal properties.

Antibodies with low isoelectric points display low levels of non-specific interactions in physiological conditions but weakly repulsive self-interactions in formulation conditions. Conversely, antibodies with high isoelectric points display highly repulsive self-interactions in formulation conditions but high levels of non-specific interactions in physiological conditions. Intermediate isoelectric points of 7.5–9 for Fv provide an attractive balance of strongly repulsive self-interactions in formulation conditions and low-to-moderate levels of non-specific binding in physiological conditions. Y-axes represents the average values from the two (A) ELISA and (B) PSP assays used to evaluate non-specific interactions. The dotted lines are defined in Fig. 4.

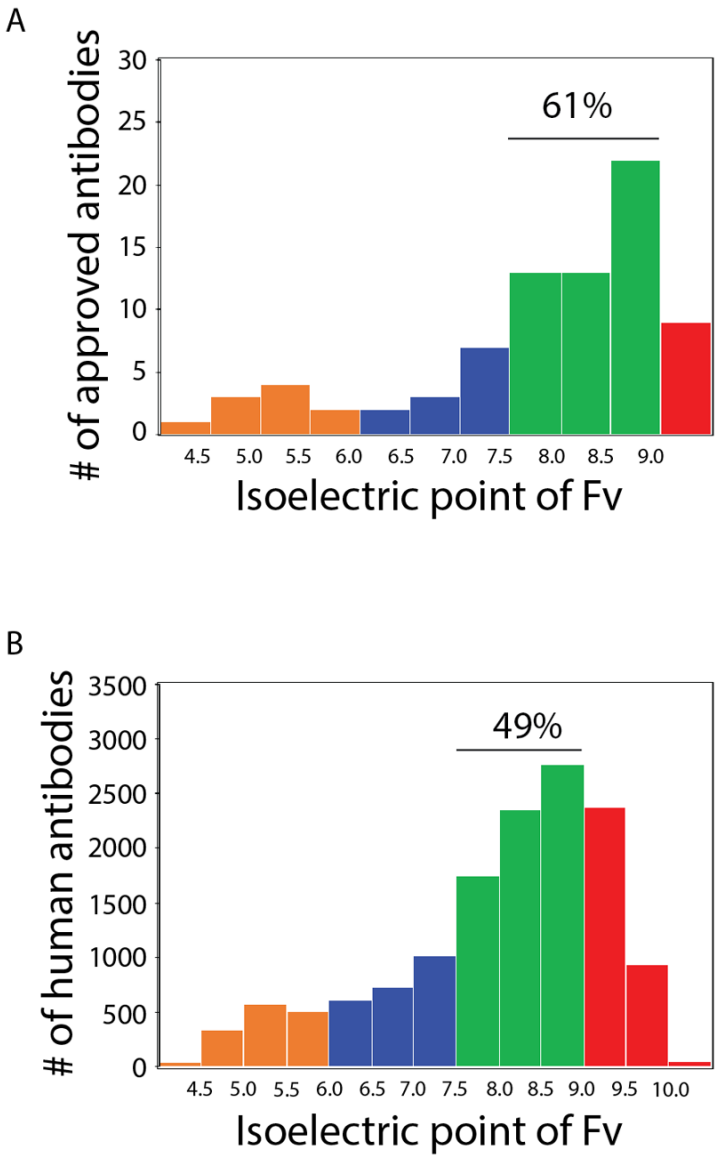

Figure 6. Distributions of Fv isoelectric for approved antibody drugs and human antibodies in general.

Distribution of Fv isoelectric points for (A) 79 approved antibodies (median pI of 8.14) and (B) 14037 human antibodies (median pI of 8.34).

Table 1.

Summary of the four clinical-stage antibodies evaluated in the study. The most homologous human germlines for the V_H and V_L domains are noted. The antibodies display a range of net charges and isoelectric points. Antibody charge values were calculated at pH 7.4 using values of −1 for Asp and Glu, +1 for Arg and Lys, and +0.1 for His.

Antibody framework	pI			Net charge (pH 7.4)			Closest human germline	
	V_H	V_L	Fv	V_H	V_L	Fv	V_H	V_L
hOKT3	9.2	9.2	9.3	5.2	4	9.2	IGHV1–46	IGKV3–20
Trastuzumab	8.0	8.6	8.6	1.1	2.1	3.1	IGHV3–66	IGKV1–39
Siltuximab	6.5	7.9	7.8	−1	1	0	IGHV3–23	IGKV3–11
Lebrikizumab	7.9	4.9	5.4	1	−2.9	−1.9	IGHV2–70	IGKV4–1

Table 2.

Summary of the heavy chain CDR3 (HCDR3) sequences used for CDR grafting in this work. The HCDR3 sequences from clinical-stage antibodies possess differences in net charge and sequence composition consisting of negatively charged (red), positively charged (blue), hydrophobic (green) and polar (black) residues. The net charges of the HCDR3 and Fv regions (pH 7.4) are calculated as described in Table 1. The muromonab HCDR3 contains a cysteine that was mutated to serine in this study.

HCDR3 #	HCDR3 amino acid sequences										Origin of HCDR3	HCDR3 net charge (pH 6)	HCDR3 net charge (pH 7.4)	Fv net charge of variants (pH 7.4)			
														hOKT3	Tras.	Silt.	Lebr.
1	**Y**	**D**	**G**	**I**	**Y**	**G**	**E**	**L**	**D**	**F**	**Carlumab**	−3	−3	9.1	2.2	−2	−2.9
2	**Y**	**Y**	**D**	**D**	**H**	**Y**	**S**	**L**	**D**	**Y**	**Muromonab***	−2.5	−2.9	9.2	2.3	−1.9	−2.8
3	**G**	**G**	**D**	**G**	**F**	**Y**	**A**	**M**	**D**	**Y**	**Trastuzumab**	−2	−2	10.1	3.2	−1	−1.9
4	**Y**	**D**	**H**	**Y**	**S**	**G**	**S**	**S**	**D**	**Y**	**Bapineuzumab**	−1.5	−1.9	10.2	3.3	−0.9	−1.8
5	**H**	**G**	**D**	**D**	**P**	**A**	**W**	**F**	**A**	**Y**	**Farletuzumab**	−1.5	−1.9	10.2	3.3	−0.9	−1.8
6	**G**	**L**	**K**	**M**	**A**	**T**	**I**	**F**	**D**	**Y**	**Seribantumab**	0	0	12.1	5.2	1	0.1
7	**S**	**L**	**A**	**R**	**T**	**T**	**A**	**M**	**D**	**Y**	**Tocilizumab**	0	0	12.1	5.2	1	0.1
8	**H**	**R**	**S**	**G**	**Y**	**F**	**S**	**M**	**D**	**Y**	**Girentuximab**	0.5	0.1	12.2	5.3	1.1	0.2
9	**R**	**Q**	**R**	**F**	**P**	**Y**	**Y**	**F**	**D**	**Y**	**Lenzilumab**	1	1	13.1	6.2	2	1.1
10	**R**	**R**	**P**	**G**	**Q**	**G**	**Y**	**F**	**D**	**F**	**Ustekinumab**	1	1	13.1	6.2	2	1.1

Table 3.

Evaluation of antibody molecular properties that are most strongly correlated with non-specific interactions in physiological conditions (PBS, pH 7.4) and self-association in formulation conditions (10 mM histidine, pH 6). The sequence-based charge features were calculated as described in Table 1. The ELISA/PSP results are for the average measurements from the four assays. The structure-based features were evaluated from Fv homology models using Molecular Operating Environment software.

Molecular Property		Region	Descriptors	ELISA #1 (pH 7.4)		ELISA #2 (pH 7.4)		PSP #1 SMP (pH 7.4)		PSP #2 OVA (pH 7.4)		ELISA/PSP (pH 7.4)		kD, mL/g (pH 6)	
			Spearman's correlation	ρ	p-value	ρ	p-value	ρ	p-value	ρ	p-value	ρ	p-value	ρ	p-value
Sequence Based	Electrostatic	HCDR3	Net charge	0.34	*	0.25	ns	0.09	ns	0.34	*	0.26	ns	0.12	ns
		CDR	Net charge	0.80	****	0.76	****	0.29	ns	0.55	***	0.69	****	0.49	*
		V_L	Net charge	0.78	****	0.79	****	0.50	**	0.46	**	0.87	****	0.76	***
		V_H	Net charge	0.77	****	0.81	****	0.32	*	0.59	****	0.68	****	0.62	*
		Fv	Net charge	0.88	****	0.89	****	0.42	**	0.55	***	0.88	****	0.86	****
		Fv	Cross charge (V_H xV_L)	0.82	****	0.75	****	0.53	**	0.53	***	0.86	****	0.63	*
		Fv	pI	0.86	****	0.83	****	0.48	*	0.56	***	0.88	****	0.84	****
		IgG	pI	0.85	****	0.84	****	0.48	*	0.56	***	0.89	****	0.84	****
Structure Based (Fv)	Stability	Fv	Buried SA (V_H/V_L interface); Å^2	−0.53	**	−0.50	**	0.26	ns	0.14	ns	−0.32	*	−0.18	ns
		Fv	Interaction energy (V_H/V_L interface); Å^2	0.59	***	0.56	**	−0.15	ns	−0.07	ns	0.40	**	0.22	ns
		Fv	Hydrophilic SA; Å^2	0.76	****	0.73	****	0.04	ns	0.16	ns	0.60	****	0.52	*
	Electrostatic	Fv	Positive patch SA; Å^2	0.82	****	0.77	****	0.37	*	0.38	*	0.82	****	0.71	**
		Fv	Negative patch SA; Å^2	−0.09	ns	0.01	ns	0.02	ns	0.11	ns	−0.16	ns	−0.20	ns
		CDR	Positive patch SA near CDR; Å^2	0.84	****	0.82	****	0.28	ns	0.40	**	0.75	****	0.60	*
		CDR	Negative patch SA near CDR; Å2	−0.08	ns	0.01	ns	0.24	ns	0.23	ns	−0.01	ns	−0.02	ns
		Fv	Dipole moment (Debye)	0.26	ns	0.30	Ns	0.27	ns	0.48	**	0.22	ns	−0.06	ns
		CDR	Net charge	0.72	****	0.67	****	−0.12	ns	0.15	ns	0.48	**	0.48	*
		Fv	Net charge	0.81	****	0.79	****	0.57	****	0.63	****	0.88	****	0.75	***
		Fv	pI	0.84	****	0.81	****	0.53	***	0.62	****	0.89	****	0.82	****

Molecular Property	Region	Descriptors	ELISA #1 (pH 7.4)		ELISA #2 (pH 7.4)		PSP #1 SMP (pH 7.4)		PSP #2 OVA (pH 7.4)		ELISA/PSP (pH 7.4)		kD, mL/g (pH 6)	
		Spearman's correlation	ρ	p-value	ρ	p-value	ρ	p-value	ρ	p-value	ρ	p-value	ρ	p-value
Hydrophobic	Fv	Zeta potential (mV)	0.81	****	0.79	****	0.57	****	0.63	****	0.88	****	0.75	***
	Fv	Hydrophobic SA; Å^2	−0.49	**	−0.48	*	−0.11	ns	−0.05	ns	−0.48	**	−0.65	*
	Fv	Hydrophobic SA; Å^2	−0.35	*	−0.37	*	−0.20	ns	−0.36	*	−0.32	*	−0.20	ns
	CDR	Hydrophobic patch SA near CDR; Å^2	−0.67	****	−0.65	****	−0.47	**	−0.42	**	−0.77	****	−0.69	**
	Fv	Hydrophobic moment	0.56	**	0.51	*	−0.27	ns	−0.14	ns	0.31	*	0.31	ns
	Fv	Hydrophobic imbalance	0.51	**	0.48	*	0.15	ns	0.00	ns	0.57	****	0.42	*

Spearman's ρ and p-values are reported, the latter which are indicated as values <0.0001 (****), <0.001 (***), <0.01 (**), 0.01 to 0.05 (*), and >0.05 (ns). Surface area is referred to as SA.